



Chapter II: Stellar atmospheres and winds

Stellar Atmospheres and Supernovae: Systematic Errors

D. John Hillier 

Department of Physics and Astronomy & Pittsburgh Particle Physics, Astrophysics and
Cosmology Center (PITT PACC), University of Pittsburgh,
3941 O'Hara Street, Pittsburgh, PA 15260, USA.
email: hillier@pitt.edu

Abstract. Over the last two decades there have been considerable advances in modelling the spectra of massive stars and supernovae (SNe). Despite this progress, there are still numerous uncertainties that affect the accuracy of models. For massive stars, convection, instabilities, clumping, and our inability to model stellar winds self-consistently likely introduce systematic errors into our analyses. For SNe, and particularly for core-collapse SNe, departures from spherical symmetry strongly affect observed spectra and need to be taken into account. There are also issues with clumping, and mixing processes (both in the progenitor and the SN explosion) that need to be resolved. For both massive stars and SNe, the accuracy and availability of atomic data continues to be an ongoing issue influencing analyses.

Keywords. line: formation, radiative transfer, stars: atmospheres, supernovae: general, stars: winds, outflows etc.

1. Introduction

Systematic errors are a major issue in many areas of astrophysics. They can be difficult to identify, and unfortunately they are generally not reduced by the addition of more data. Systematic errors can arise from many sources: Model assumptions, errors in the analysis code, systematic errors in the observational data, errors in the atomic data, and personal biases.

Some of the most infamous cases of systematic errors relate to distances. For example, early determinations of the size of the Galaxy were biased because it was not appreciated that there were two types of pulsating variables: classical cepheids (associated with Pop I stars) and RR Lyrae stars (associated with Pop II stars). Determinations of the Hubble constant have been plagued by systematic errors, and it is possible that the current difference between the Hubble constant determined via Planck, and that found using Cepheid variables, could be due to systematic errors (e.g., [Freedman et al. 2019](#); [Freedman 2021](#) but see [Riess et al. 2022](#)).

With respect to stars, we highlight issues with fitting the He I singlet and triplet lines, particularly in O supergiants. For a long time it was generally argued that the problem was with the triplet lines, and it was thought to arise from a dilution effect (e.g., [Voels et al. 1989](#)). However, it is now known that the problem is with the singlet lines. and occurs because weak Fe lines overlap with the He I singlet resonance transition at 584.334 Å ([Najarro et al. 2006](#)). The Fe lines remove photons from the singlet transition, lowering the $2p\ ^1P^o$ population, and hence altering the strength of singlet transitions – particularly those ending on the $2p\ ^1P^o$ state ([Najarro et al. 2006](#)).

A more minor effect is associated with rotational broadening. Generally rotational broadening is taken into account using a convolution technique (e.g., Gray 2008), and for most absorption features in O stars this is an excellent approximation. However this technique does not work for wind lines (since the rotation velocity falls with distance from the star, and since the outflow is not purely radial) and can fail for some photospheric lines. For example, in ζ Puppis several weak emission lines show double-peaked emission profiles (e.g., N IV λ 4058). These cannot be explained using the normal convolution technique, and their existence was used to invoke large-scale co-rotating structures (De Becker et al. 2009). However the double-peaked profiles are automatically produced when rotational broadening is computed from first principles. It occurs in ζ Puppis because non-LTE effects cause these weak photospheric emission lines to be limb brightened (Hillier et al. 2012).

This paper is organized as follows. We briefly discuss some issues with the analysis of massive stars and their winds in §2. An alternative approach for treating clumping in stellar wind models is described in §2.1, while in §2.2 we discuss mass-loss rate determinations. In §3 we turn our attention to core-collapse SNe, and discuss three sources of systematic errors – progenitors (§3.1), chemical mixing (§3.2), and molecular cooling (§3.3). Conclusions can be found in §4.

2. Massive stars & stellar winds: Systematic errors

In classical analyses of massive stars, the star and its wind are generally assumed to be spherical. The wind, originally assumed to be homogeneous, is now understood to be clumped, and this is treated by approximate methods. The presence of significant rotation in many stars immediately indicates that the winds are unlikely to be spherically symmetric. This can be important for interpreting P Cygni profiles since the absorption component samples only along our line of sight to the star (and hence samples only a small volume of wind) while the emission component samples most of the wind. When discrepancies in fitting P Cygni profiles occur, they are normally attributable to wind clumping and porosity.

Both observational (e.g., Eversberg et al. 1998; Prinja & Massa 2010; Hillier & Miller 1999; Crowther et al. 2002) and theoretical studies (e.g., Owocki et al. 1988; Sundqvist & Owocki 2013) indicate that the winds are inhomogeneous with significant spatial and angular variations in wind speed and density. The inhomogeneities are generally thought to arise from the line-driven instability, but other processes, such as convection and non-linear pulsations, may act as seeds.

Since different radiative processes have a different functional dependence on density, the influence of clumping is not uniform. In particular, electron scattering, and the strength of unsaturated P Cygni profiles arising from the dominant ionization state, will scale with density, while recombination processes and free-free emission scale with the square of the density.

In addition, inhomogeneities mean that wind porosity (Oskinova et al. 2007) and vorosity (Owocki 2008) need to be included in models. Porosity arises from the spatial dependence of clumping, and occurs when some sight lines have a significantly lower optical depth because they primarily pass through material of low density. Vorosity (a term coined by Stan Owocki) occurs because some directions may have very little material at certain velocities, and hence this material is transparent to line radiation (Owocki 2008) at these velocities. Porosity affects both lines and the continuum, whereas vorosity only affects line transfer. Due to vorosity, clumps can introduce structure into the absorption component along a single sight line (Fig. 1). The structure can/will disappear when an average is taken over many sight lines but it can affect doublet line ratios

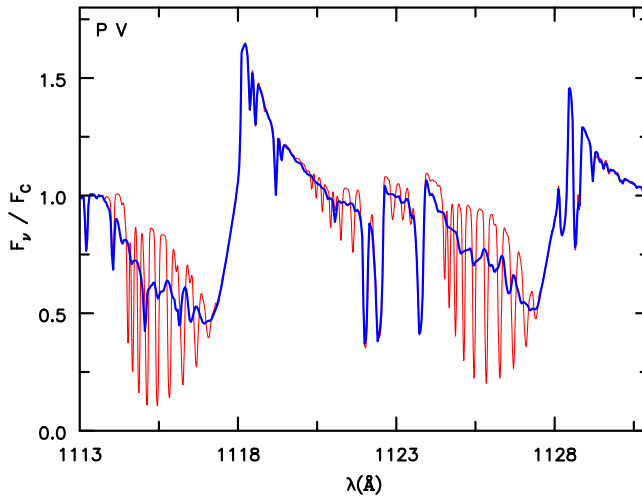


Figure 1. An illustration of the P V $\lambda\lambda 1117, 1128$ profile in a model for AzV83. The red curve shows the profile computed using the shell model. Because the shells have a distinct velocity, the P Cygni absorption profile presents a comb-like structure which is not observed. However, when we allow the shells to have a slightly different radial velocity along different sight lines we get a smooth profile, much like that observed. Reproduced from: “Using Shell models to investigate clumping in the wind of the O7Iaf+ supergiant AzV83” (figure 4), Flores & Hillier (2021).

(e.g. Massa et al. 2003). Through the study of doublet ratios it is possible to place constraints on the amount of wind porosity/vorosity (Prinja & Massa 2013).

Another important, potential cause of systematic errors is hot gas and its X-ray emission. O stars are significant X-ray emitters with $L_x/L_{\text{BOL}} \sim 10^{-7}$ to 10^{-6} (e.g., Cassinelli & Swank 1983; Chlebowksi 1989). These X-rays, through Auger ionization, affect the ionization structure of the wind, and are responsible for the so-called superior† P Cygni profiles (e.g., O VI) in O stars (e.g., Cassinelli & Olson 1979). The X-ray emission is thought to arise from shocks produced by the line-driven instability (Lucy & White 1980; Feldmeier et al. 1997). In most modelling the X-ray emission is simply added as an extra wind-emission source, with several ad hoc parameters defining the shock temperature and emissivity as a function of location. The shock structure, and the coupling between the shocks and their associated hot gas, and the cooler wind, is ignored.

2.1. Clumping

In most studies clumping is treated using a volume-filling-factor (VFF) approach. A fraction, f , of the spherical wind is assumed to consist of small clumps while the remaining fraction is devoid of material. With this assumption it is easy to modify standard radiative transfer codes to incorporate clumping. However the approach assumes that the interclump medium is void, that the density at a given radius is homogeneous, and that the clumps are small – all assumptions are invalid “at some level”, but their influence on results is generally unknown. Further, the radial dependence of f is described by several parameters, which are difficult to constrain.

Extensions to the VFF approach have been developed that allow for an interclump medium, and both porosity and vorosity (e.g., Sundqvist et al. 2014). These techniques are also approximate, require additional free parameters, and can still lead to systematic errors in inferred wind parameters.

† An ion whose presence cannot be explained by the photospheric radiation field.

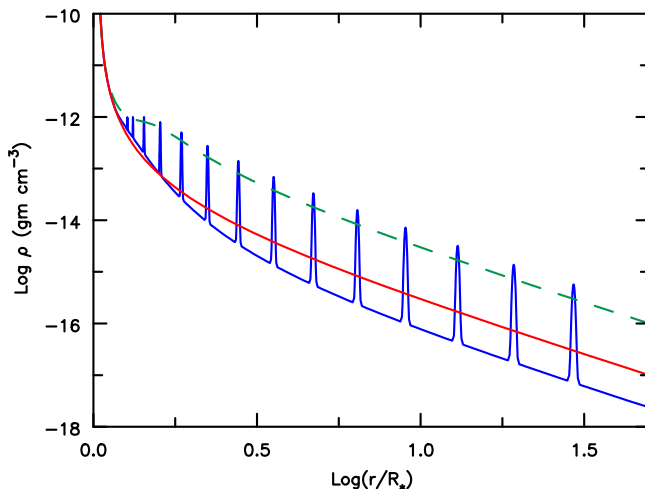


Figure 2. An illustration of the density distribution in three models for AzV83 – all models have the same average mass-loss rate. The red solid curve is for a smooth density distribution and the blue solid curve is for the shell model with an average wind VFF of 0.1. The green dashed curve illustrates the clump density in the VFF model (but recall that the interclump medium is void) with VFF = 0.1. By adjusting model parameters it is possible to vary the number of clumps, clump size and the density of the interclump medium. Reproduced from: “Using Shell models to investigate clumping in the wind of the O7Iaf+ supergiant AzV83” (figure 3), Flores & Hillier (2021).

One way to test the influence of assumptions is to invoke an alternative model which allows for clumping but is based on different assumptions. One such approach is to assume that the star consists of spherical dense shells (shell model) (e.g., Hillier 1991a; Flores & Hillier 2021; Flores & Hillier 2022), as illustrated in Fig. 2. In this approach the finite size of the clumps, the interclump medium, and vorosity can be treated. However it is also unlikely to be valid – it does not allow for non-monotonic velocity fields and the assumption of spherical shells is invalid – they will be broken up on some angular scale.

The shell model has been applied to two stars – AzV83 (an O7Iaf+ supergiant) (Flores & Hillier 2021) and HD 50896 (a classical WN4 star) (Flores & Hillier 2022). In these models the shell structure is set to yield a pre-specified VFF, with the number of shells a free parameter. Typically the shells have a radial thickness of order the Sobolev length ($= rV_D/V$ where V_D is the line Doppler width).

For AzV83 results obtained with the shell model, and the VFF approach, are similar (Flores & Hillier 2021). A slightly higher mass loss ($\sim 30\%$) is needed in the shell model, an effect also seen in an earlier study that used a more realistic treatment of clumping (Sundqvist et al. 2011). The shells produce highly structured P Cygni absorption components, but the structure averages out if we assume that the shells have small angular variations in velocity (effectively equivalent to breaking the shells up in angle, and performing a slight shift in radial location) when we do a formal solution to compute observed spectra. As the model allows for the interclump medium, the shell model, unlike the VFF model, reproduces the O VI $\lambda\lambda$ 1032, 1038 line in AzV83 for a reasonable X-ray flux. The importance of the interclump medium for explaining superions in O star spectra was previously demonstrated by Zsargó et al. (2008).

By contrast, when applied to HD 50896 the shell models failed to match the He II line strengths – the emission profiles contain a central absorption component and appear double-peaked (Fig. 3). This is attributable to optical depth effects. For lines of sight passing through the shell center, photon escape in a line is substantially influenced by

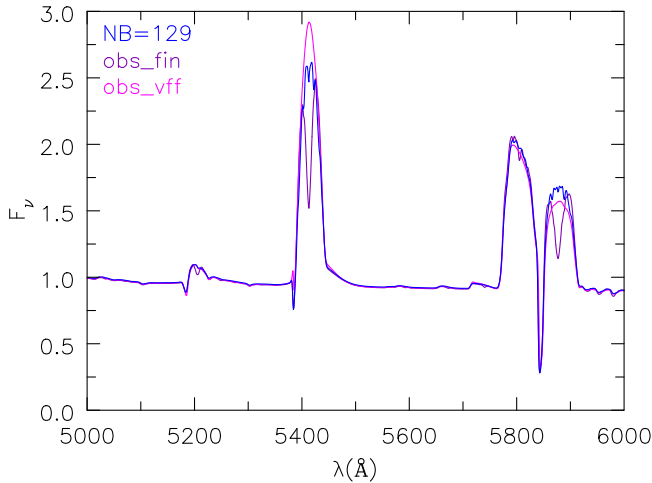


Figure 3. Illustration of how a pure shell model with complete shells (purple curve) fails to produce the He II emission strengths. When the shells are broken up (blue curve), there is much better agreement with the VFF results (pink curve). Full details can be found in Flores & Hillier (2022).

the width of the shell. However for lines of sight through the limb of the shell, the path length is much longer, minimizing the influence of the shell thickness on photon escape, and greatly reducing photon escape in the lines. Continuum formation is much less affected since the scale length for a continuum photon to escape is much larger than for photon escape in a line.

Better consistency can be achieved with the VFF approach if we break the shells up in angle, and randomly distribute each “partial” shell over a radial distance of approximately $\delta r/2$ where δr is the shell separation. Our results argue that the lateral scale of the shells must be small – less than 1° .

2.2. Mass-loss rates and the velocity law

Typically the mass-loss rate and velocity law are assumed, with the velocity law (above the sonic point) parameterized by several free parameters. The mass-loss rate and velocity law are then constrained through spectral fitting, although in many cases the constraints on the shape of the velocity law are weak. Unfortunately, it is difficult to determine the mass-loss rate uniquely, since assumptions about both clumping and porosity/vorosity will affect its determination. When porosity/vorosity effects are ignored, f can be constrained by fitting both $H\alpha$ and P V $\lambda\lambda 1117, 1128$ in O stars, while in Wolf-Rayet (WR) stars constraints on f come from a comparison of emission line strengths with their associated electron scattering wings. Obviously our biases about clumping, and (in many cases) the neglect of porosity/vorosity effects will introduce systematic errors into mass-loss rate determinations – the significance of such errors remains to be seen.

A major issue for Wolf-Rayet stars is connecting derived radii and effective temperatures with those of evolutionary models (e.g., Groh et al. 2014). For most WR stars the observed radiation originates in the wind, and is thus insensitive to the radius and effective temperature of the star defined at the sonic point (e.g., Hillier 1991b). Consequently, observationally derived values depend on the assumed velocity law.

Ideally we would like to deduce the velocity law and mass-loss rate from hydrodynamic calculations. Such calculations would be 3D, allow for stellar rotation, and be time dependent (e.g., Moens et al. 2022). Work towards this goal is in progress, but

researchers face many hurdles. One-D hydrodynamical models are routinely constructed, but these typically assume a clumping structure. For some stars these 1D solutions appear to give reasonable answers while for others there appears to be significant discrepancies between the mass-loss rates and terminal velocities deduced from 1D hydrodynamic solutions, and those inferred from an analysis of the observations (e.g., [Sundqvist et al. 2019](#); [Gormaz-Matamala et al. 2021](#)).

3. Core-collapse supernovae: The final stage of massive star evolution

An understanding of core-collapse SNe is crucial for many areas of astrophysics. SNe influence the interstellar and intergalactic medium through the deposition of momentum, energy, and chemically enriched material and thus influence star formation and galactic evolution, and create/distribute the elements necessary for life. Many questions remain unanswered, particularly related to how core-collapse SNe explode. It is only with the development of complex 3D models that explosions of massive stars can be fully explored (e.g., [Wongwathanarat 2017](#)).

Whatever the exact mechanism, core-collapse SNe are intrinsically aspherical. Direct evidence for asphericity comes from polarization observations (e.g., [Cropper et al. 1988](#); [Wang et al. 1996](#); [Kawabata et al. 2002](#)), and line profile analyses (e.g., [Hanuschik & Dachs 1987](#); [Chugai 2007](#)). Observed SN remnants also show evidence for strong asymmetric explosions. However most modelling of SN light curves and spectra assumes spherical symmetry. The primary reason is computational – it is prohibitively expensive to compute a significant set of time-dependent non-LTE models in 3D, even with approximations. It should also be stressed that the departures from sphericity are unlikely to be described by a simple axi-symmetric model. Theoretical models show complex asymmetries (e.g., [Hammer et al. 2010](#); [Janka et al. 2007](#)).

3.1. Progenitor issues

Understanding SN explosions requires a detailed progenitor model. However the evolution of massive stars is in itself uncertain, and this will translate into uncertainties in explosion models, and the deduced supernova properties. Uncertainties in massive star properties were recently emphasized in a study by [Agrawal et al. \(2022\)](#) who found that the differences in model results increase with stellar mass, primarily as a consequence of how instabilities associated with the star's proximity to the Eddington limit are treated. An illustration of the different evolutionary tracks they obtained with different evolutionary codes is shown in [Fig. 4](#). Other major uncertainties affecting stellar evolution calculations arise from the adopted mass-loss rates, and the treatment of convection and rotation.

Given the uncertainties in the theoretical treatment of stellar evolution, and uncertainties in mass-loss rates, inferring the progenitor properties, such as its mass on the zero-age main sequence, from the SN ejecta properties is very difficult (e.g., [Dessart & Hillier 2019](#)). While mass is obviously the most fundamental parameter that influences a star's evolution, other factors such as metallicity, initial rotation rate, and whether the star's evolution has been influenced by interactions with a companion (which may no longer be present in the system) are also crucial (e.g., [Farrell et al. 2020](#)). In principle, mass loss, which can substantially influence a star's evolution, can be deduced from stellar properties at that instant, but in practice evolutionary codes use descriptive formulae with several free parameters. These, of course, introduce systematic errors into an evolutionary calculation. In massive stars one of the more problematic issues is eruptive mass loss. This phenomenon is not understood, and is generally ignored.

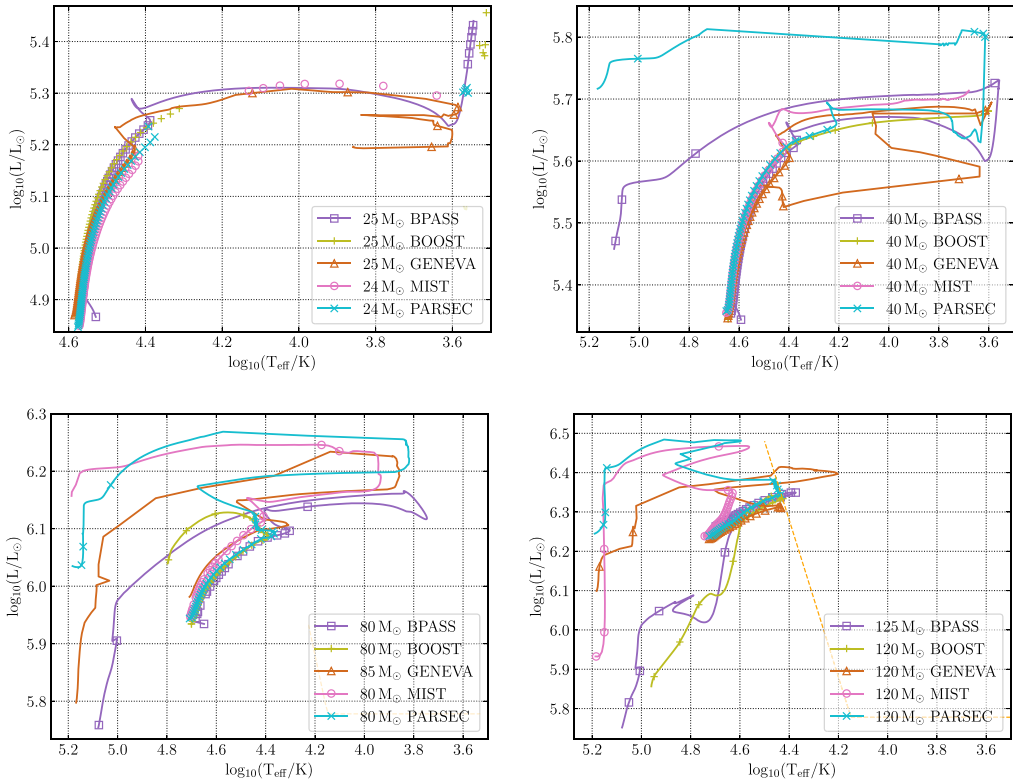


Figure 4. An illustration of the different evolutionary tracks for four ZAMS masses computed using different evolutionary codes. As clearly evident, there is a great deal of dispersion in the evolutionary tracks, particularly at large masses. Reproduced from: “Explaining the differences in massive star models from various simulations” (figure 1), [Agrawal et al. \(2022\)](#).

3.2. Mixing of Ca into the O zone

A major problem in modelling core-collapse SNe with 1D models relates to their chemical composition. Stellar evolution calculations for the massive progenitors of core-collapse SNe predict an “onion-like” structure for the chemical composition (see Fig. 6). However in 3D calculations of SN explosions, significant radial mixing of the material occurs (e.g., [Janka et al. 2007](#); [Hammer et al. 2010](#)). This mixing is macroscopic – the radially mixed material retains its initial chemical composition. Thus, for example, there is no H in the O-rich material even though their distributions in velocity (or equivalently, radius) overlap.

In 1D modeling, a naive approach for treating mixing would be to run a smoothing function through the material. This causes microscopic mixing and that will/can introduce severe biases into spectroscopic modelling. This occurs because the cooling of the ejecta is determined by its chemical composition, and the cooling efficiency varies widely between different chemical species (and between different ionization stages). A striking illustration of the effect occurs with Ca and Si cooling.

With the smoothing approach, we microscopically mix Ca from the Si-rich shell into the O-rich shell. However, Ca II $\lambda\lambda$ 7291, 7233 is a much more efficient coolant than O I $\lambda\lambda$ 6300, 6364, and consequently a small amount of Ca in the O zone can dramatically weaken the strength of O I $\lambda\lambda$ 6300, 6364 (e.g., [Fransson & Chevalier 1989](#); [Dessart & Hillier 2020a](#)). The effect, illustrated in Fig. 5, is of crucial importance since the mass of O in

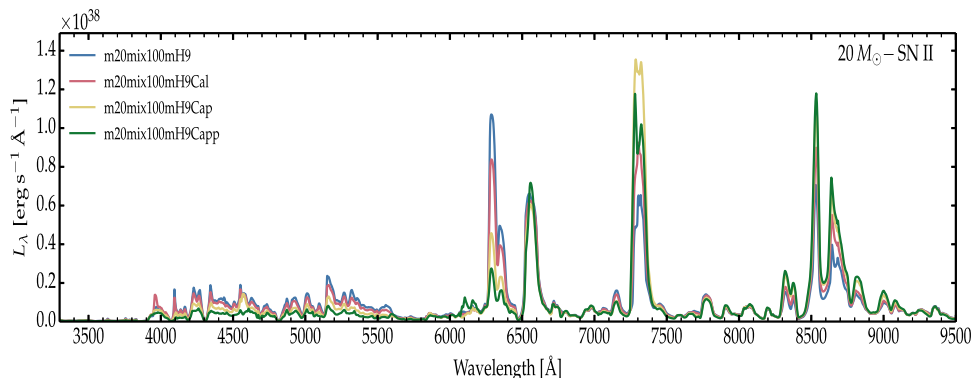


Figure 5. An illustration of the influence of mixing Ca into the O zone of nebular phase spectra. Successive models vary by a factor of 10 in mass fraction and have $X(\text{Ca}) = 7 \times 10^{-5}$ (blue), 7×10^{-4} (red), 7×10^{-3} (yellow) and 7×10^{-2} (green). As the Ca to O ratio increases, the O I $\lambda\lambda$ 6300, 6364 emission is depressed, and the Ca II $\lambda\lambda$ 7291, 7233 emission enhanced. Reproduced from: “Radiative-transfer modeling of nebular-phase type II supernovae. Dependencies on progenitor and explosion properties” (figure 7), [Dessart & Hillier \(2020a\)](#).

the ejecta varies strongly with the progenitor mass ([Woosley et al. 2002](#)), and hence is used as a diagnostic probe of the progenitor mass (e.g., [Jerkstrand et al. 2012](#)).

The influence of Ca on the O line strengths has been known for a long time. In some Kepler models ([Ensmann & Woosley 1988](#)), pollution of the O-rich shell by the Si-rich shell meant that the models could not explain the observed line strengths in SN 1987A ([Fransson & Chevalier 1989](#)). An extensive study of convective oxygen and silicon burning shells in supernova progenitors, and shell mixing, was undertaken by [Collins et al. \(2018\)](#). This problem of shell merging and mixing in progenitor modelling has not been fully solved – it still occurs in some evolutionary calculations (although it can be artificially suppressed), and it is unknown as to what extent it occurs in nature. In some cases, shell merging can occur just prior to collapse, and it is possible that the short time-scale (e.g., 10 minutes before collapse) means that the merging is incomplete when core collapse occurs ([Collins et al. 2018](#)).

To treat macroscopic mixing [Dessart & Hillier \(2020b\)](#) developed an approach in which the shells in the original model are broken up into several pieces, and these are then distributed in radius/velocity (Fig. 6). Importantly, this approach preserves the distinct chemical composition of the shells.

3.3. Cooling by Molecules

Molecular cooling in core-collapse SN ejecta is known to be important (e.g., [Cherchneff & Sarangi 2011](#); [Matsuura 2017](#); [Rho et al. 2021](#)). In SN 1987A, emission in the first overtone of CO was seen in spectra at day 137 and the fundamental band was a contributor to excess emission seen in the M band ([Catchpole et al. 1988](#)). Modelling of CO emission in SN ejecta is difficult since it is necessary to solve the chemical reaction equations producing and destroying CO (i.e., chemical equilibrium cannot be assumed). Unfortunately many of the reaction rates are poorly known, or only available at temperatures not relevant to SN ejecta. It is also likely that the vibrational levels are not in local thermodynamic equilibrium, requiring that their populations be deduced from the solution of the kinetic equations. To construct the kinetic equations we need collision rates, which are also poorly known.

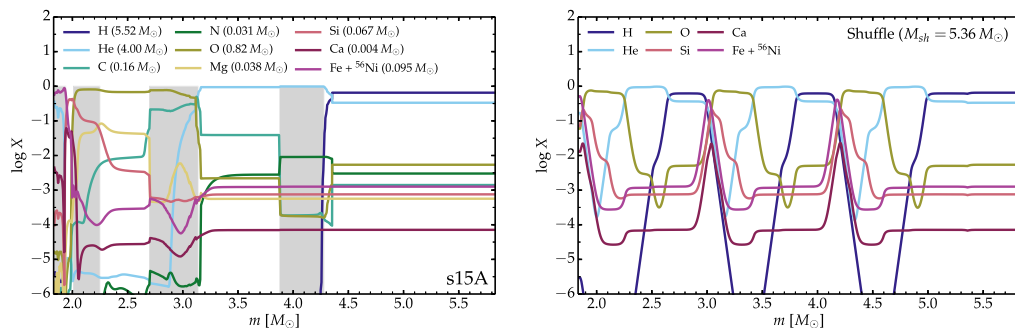


Figure 6. An illustration of the treatment of macroscopic mixing in 1D. On the left we see the chemical composition of the original SN model (based on the S15A ejecta model of Woosley & Heger (2007)) – the onion-like chemical structure of the ejecta is clearly evident. On the right the distinct chemical zones have been broken into three fragments, and these have then been shifted in radius. See Dessart & Hillier (2020b) for further details. Reproduced from: “Radiative-transfer modeling of supernovae in the nebular-phase. A novel treatment of chemical mixing in spherical symmetry” (figure 1), Dessart & Hillier (2020b).

CO formation has been introduced (Liljegren et al. 2020) into SUMO, the SN modelling code of Anders Jerskstrand (Jerkstrand et al. 2011). More recently SiO was included, and the code modified to allow the vibrational levels to be treated in non-LTE (Liljegren et al. 2022).

PhD student, Collin McLeod, is currently installing molecules into CMFGEN. For the solution of the chemical equations we treat (in addition to the associated atomic species) CO, CO⁺, C₂, C₂⁺, O₂, O₂⁺, CO₂, CO₂⁺, C₂O, and C₂O⁺, however only the opacities and emissivities of CO are allowed for when determining the temperature structure of the ejecta. We currently treat CO in LTE, but we plan to relax this assumption in the near future – we also plan to include SiO.

Due to the complexities of cooling in SN ejecta, we have had difficulties in obtaining converged models. Initial results confirm the importance of CO cooling, and its potential impact on SN spectra. In Fig. 7 we show the influence of CO cooling on the optical spectrum for a model roughly applicable to SN 1987A. While this model overemphasizes the importance of CO cooling, it does demonstrate that significant potential errors may occur in fitting optical spectra if cooling by CO and other molecules is neglected. In turn, these erroneous fits may lead to an incorrect estimate of the oxygen mass, and hence the mass of the progenitor that gave rise to the SN.

4. Conclusions

Systematic errors are hard to identify, are hard to quantify, and arise from many sources. Before drawing any conclusions, it is important to investigate possible sources of systematic errors that may influence conclusions.

An obvious potential source of systematic errors arise in codes designed to perform theoretical modeling. All these codes have underlying assumptions that can have a profound influence on their results. In many cases these assumptions are necessary, but they must be considered when drawing conclusions, and tests should be made to examine their applicability. A potential problem with today’s codes is that many have an extensive development history. Assumptions valid at one time may no longer be valid when changes are made to the code. We found such issues when installing molecules into CMFGEN.

When using public codes please provide feedback to the developers. Such feedback is important for further code development.

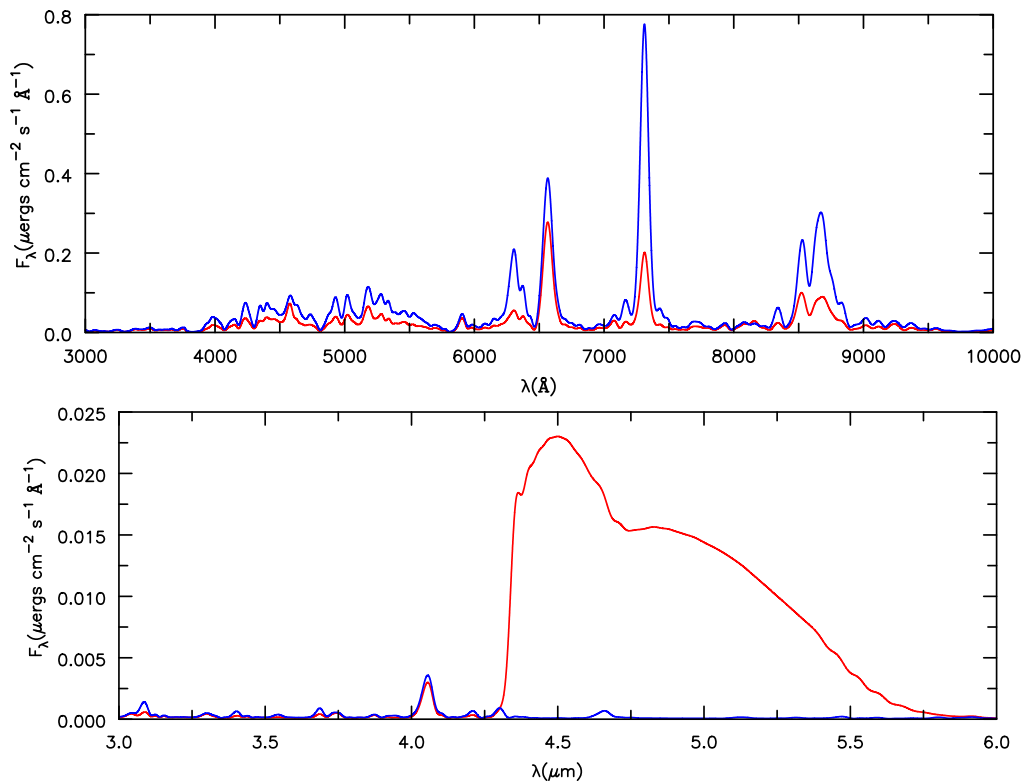


Figure 7. Spectra for a model of a supernova similar to SN 1987A. The model has classical mixing (i.e., not the shell approach). The blue line shows the spectrum at an age of 330 days without cooling, while the (preliminary) model shown in red has CO cooling. CO cooling, primarily by the fundamental band, weakens optical features such as O I $\lambda\lambda$ 6300, 6364, Ca II $\lambda\lambda$ 7291, 7233, and Ca II $\lambda\lambda$ 8498, 8542, 8662. Longward of $4.3\ \mu\text{m}$ we see the strong emission by the fundamental band of CO which completely dominates this spectral region.

References

- Agrawal, P., Szécsi, D., Stevenson, S., Eldridge, J. J., & Hurley, J. 2022, *MNRAS*, 512, 5717
 Cassinelli, J. P. & Olson, G. L. 1979, *ApJ*, 229, 304
 Cassinelli, J. P. & Swank, J. H. 1983, *ApJ*, 271, 681
 Catchpole, R. M., Whitelock, P. A., & Feast, M. W., et al. 1988, *MNRAS*, 231, 75P
 Cherchneff, I. & Sarangi, A. 2011, in *The Molecular Universe*, ed. J. Cernicharo & R. Bachiller, Vol. 280, 228–236
 Chlebowski, T. 1989, *ApJ*, 342, 1091
 Chugai, N. N. 2007, in *AIP Conf. Ser.*, Vol. 937, *Supernova 1987A: 20 Years After: Supernovae and Gamma-Ray Bursters*, ed. S. Immler, K. Weiler, & R. McCray, 357–364
 Collins, C., Müller, B., & Heger, A. 2018, *MNRAS*, 473, 1695
 Cropper, M., Bailey, J., McCowage, J., Cannon, R. D., & Couch, W. J. 1988, *MNRAS*, 231, 695
 Crowther, P. A., Hillier, D. J., & Evans, C. J., et al. 2002, *ApJ*, 579, 774
 De Becker, M., Rauw, G., & Linder, N. 2009, *ApJ*, 704, 964
 Dessart, L. & Hillier, D. J. 2019, *A&A*, 625, A9
 —. 2020a, *A&A*, 642, A33
 —. 2020b, *A&A*, 643, L13
 Ensmann, L. M. & Woosley, S. E. 1988, *ApJ*, 333, 754
 Eversberg, T., Lépine, S., & Moffat, A. F. J. 1998, *ApJ*, 494, 799
 Farrell, E. J., Groh, J. H., Meynet, G., & Eldridge, J. J. 2020, *MNRAS*, 494, L53

- Feldmeier, A., Kudritzki, R. P., Palsa, R., Pauldrach, A. W. A., & Puls, J. 1997, *A&A*, 320, 899
- Flores, B. L. & Hillier, D. J. 2021, *MNRAS*, 504, 311
- , 2022, *MNRAS*, submitted
- Fransson, C. & Chevalier, R. A. 1989, *ApJ*, 343, 323
- Freedman, W. L. 2021, *ApJ*, 919, 16
- Freedman, W. L., Madore, B. F., & Hatt, D., et al. 2019, *ApJ*, 882, 34
- Gormaz-Matamala, A. C., Curé, M., & Hillier, D. J., et al. 2021, *ApJ*, 920, 64
- Gray, D. F. 2008, *The Observation and Analysis of Stellar Photospheres* (Cambridge Uni. Press)
- Groh, J. H., Meynet, G., Ekström, S., & Georgy, C. 2014, *A&A*, 564, A30
- Hammer, N. J., Janka, H.-T., & Müller, E. 2010, *ApJ*, 714, 1371
- Hanuschik, R. W. & Dachs, J. 1987, *A&A*, 182, L29
- Hillier, D. J. 1991a, *A&A*, 247, 455
- Hillier, D. J. 1991b, in *IAU Symposium*, Vol. 143, *Wolf-Rayet Stars and Interrelations with Other Massive Stars in Galaxies*, ed. K. A. van der Hucht & B. Hidayat, 59
- Hillier, D. J., Bouret, J.-C., Lanz, T., & Busche, J. R. 2012, *MNRAS*, 426, 1043
- Hillier, D. J. & Miller, D. L. 1999, *ApJ*, 519, 354
- Janka, H.-T., Langanke, K., Marek, A., Martínez-Pinedo, G., & Müller, B. 2007, *Phys. Rep.*, 442, 38
- Jerkstrand, A., Fransson, C., & Kozma, C. 2011, *A&A*, 530, A45+
- Jerkstrand, A., Fransson, C., Maguire, K., Smartt, S., Ergon, M., & Spyromilio, J. 2012, *A&A*, 546, A28
- Kawabata, K. S., Jeffery, D. J., Iye, M., & et al. 2002, *ApJL*, 580, L39
- Liljegren, S., Jerkstrand, A., Barklem, P. S., Nyman, G., Brady, R., & Yurchenko, S. N. 2022, arXiv e-prints, arXiv:2203.07021
- Liljegren, S., Jerkstrand, A., & Grumer, J. 2020, *A&A*, 642, A135
- Lucy, L. B. & White, R. L. 1980, *ApJ*, 241, 300
- Massa, D., Fullerton, A. W., Sonneborn, G., & Hutchings, J. B. 2003, *ApJ*, 586, 996
- Matsuura, M. 2017, *Dust and Molecular Formation in Supernovae*, ed. A. W. Alsabti & P. Murdin (Springer, Cham.), 2125
- Moens, N., Poniatoski, L. G., Hennicker, L., Sundqvist, J. O., El Mellah, I., & Kee, N. D. 2022, arXiv e-prints, arXiv:2203.01108
- Najarro, F., Hillier, D. J., Puls, J., Lanz, T., & Martins, F. 2006, *A&A*, 456, 659
- Oskinova, L. M., Hamann, W.-R., & Feldmeier, A. 2007, *A&A*, 476, 1331
- Owocki, S. P. 2008, in *Clumping in Hot-Star Winds*, ed. W.-R. Hamann, A. Feldmeier, & L. M. Oskinova (Potsdam: Univ.-Verl), 121
- Owocki, S. P., Castor, J. I., & Rybicki, G. B. 1988, *ApJ*, 335, 914
- Prinja, R. K. & Massa, D. L. 2010, *A&A*, 521, L55
- , 2013, *A&A*, 559, A15
- Rho, J., Evans, A., Geballe, T. R., & Banerjee, D. P. K., et al. 2021, *ApJ*, 908, 232
- Riess, A. G., Yuan, W., & Macri, Lucas M., et. al. 2022, *ApJL*, 934, L7
- Sundqvist, J. O., Björklund, R., Puls, J., & Najarro, F. 2019, *A&A*, 632, A126
- Sundqvist, J. O. & Owocki, S. P. 2013, *MNRAS*, 428, 1837
- Sundqvist, J. O., Puls, J., Feldmeier, A., & Owocki, S. P. 2011, *A&A*, 528, A64+
- Sundqvist, J. O., Puls, J., & Owocki, S. P. 2014, *A&A*, 568, A59
- Voels, S. A., Bohannan, B., Abbott, D. C., & Hummer, D. G. 1989, *ApJ*, 340, 1073
- Wang, L., Wheeler, J. C., Li, Z., & Clocchiatti, A. 1996, *ApJ*, 467, 435
- Wongwathanarat, A. 2017, in *Supernova 1987A:30 years later - Cosmic Rays and Nuclei from Supernovae and their Aftermaths*, ed. A. Marcowith, M. Renaud, G. Dubner, A. Ray, & A. Bykov, Vol. 331, 101–106
- Woosley, S. E. & Heger, A. 2007, *Phys. Rep.*, 442, 269
- Woosley, S. E., Heger, A., & Weaver, T. A. 2002, *Reviews of Modern Physics*, 74, 1015
- Zsargó, J., Hillier, D. J., Bouret, J.-C., Lanz, T., Leutenegger, M. A., & Cohen, D. H. 2008, *ApJL*, 685, L149

Acknowledgements

Partial support from STScI theory grant HST-AR-16131.001-A (DJH) and Astrophysical theory grant 80NSSC20K0524 is acknowledged. STScI is operated by the Association of Universities for Research in Astronomy, Inc., under NASA contract NAS 5-26555. Special thanks to my students, Brian Flores and Collin McLeod, for allowing me to use their work in this review.

Discussion

Unknown: In the supernova model, how much Ca has been mixed into the O zone?

D. John Hillier: The 1987A model is an old model and uses microscopic mixing. The O/Ca ratio is roughly 300 to 1 in the O-rich material, and it is probable that the level of mixing used causes an overestimate of the importance of CO cooling.

Unknown: You mentioned shocks and X-rays in your talk. A lot of supernovae that appear normal may have shocks arising from the interaction with circumstellar material. Is it possible to incorporate a little bit of X-ray emission into your ejecta?

D. John Hillier: It is easy to include the influence of X-rays if we simply specify a level of X-ray emission through the ejecta – this is already done in models for O and Wolf-Rayet stars. Low levels of X-rays are probably not crucial since we already have γ -rays in the model, and we account for the influence on level populations by the non-thermal electrons that are produced by these γ -rays. We also have run models where we have used CMFGEN to post process (with a fixed temperature) hydrodynamic models where the ejecta has interacted with circumstellar material. More recently we are considering models in which we simply dump energy into the the outer region of the ejecta. None of these approaches are fully satisfactory, but they do give insights into the fluxes and spectra produced by interstellar interactions.